

Probe Report

Title: Discovery, SAR, and Biological Evaluation of a Non-Inhibitory Chaperone for Acid Alpha Glucosidase

Authors: Juan J. Marugan^{a*}, Wei Zheng^a, Marc Ferrer^a, Omid Motabar^{a,b}, Noel Southall^a, Ehud Goldin^b, Wendy Westbrook^b, and Ellen Sidransky^b

^a NIH Chemical Genomics Center, National Human Genome Research Institute, National Institutes of Health, 9800 Medical Center Drive, Rockville, MD, 20850, United States.

^b Medical Genetics Branch, National Human Genome Research Institute, National Institutes of Health, Building 35 Rm1A213, 35 Convent Drive, Bethesda, Maryland 20892, United States.

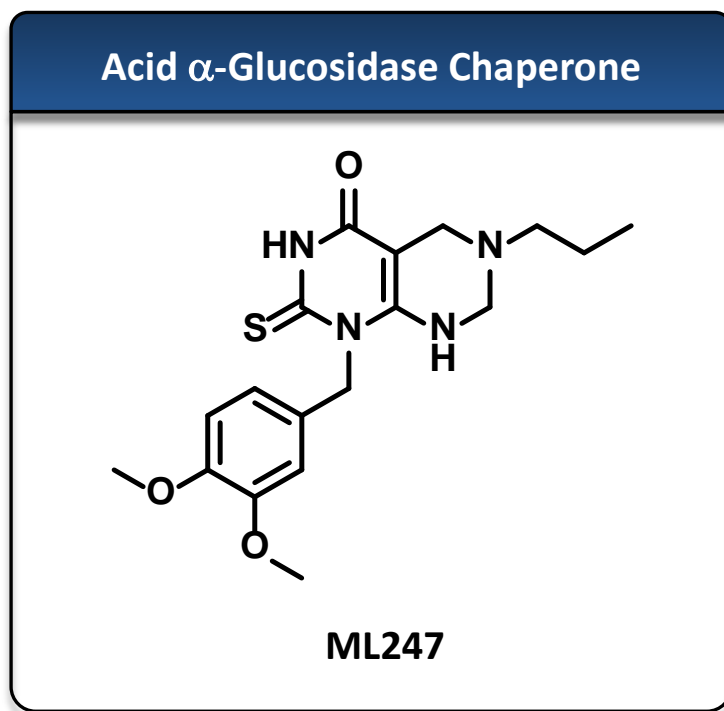
* To whom correspondence should be addressed: Email: maruganj@mail.nih.gov

Screening Center Name & PI: NIH Chemical Genomics Center, Christopher P. Austin
Chemistry Center Name & PI: NIH Chemical Genomics Center, Christopher P. Austin
Assay Submitter & Institution: Wei Zheng, NIH Chemical Genomics Center
PubChem Summary Bioassay Identifier (AID): 1473

Abstract

Glycogen storage disease II, or Pompe disease, is a rare and often fatal autosomal recessive lysosomal storage disorder (LSD) caused by the dysfunction of the lysosomal enzyme acid alpha-glucosidase (GAA). Accumulation of GAA's substrate, glycogen, causes enlargement of cellular lysosomes, adversely affecting many cells, especially heart and skeletal muscle tissues. The only FDA approved treatment for Pompe disease is enzyme replacement therapy, called Myozyme, which has significant limitations. Importantly, of the over 100 different mutations known to cause Pompe disease, many retain enzymatic activity *in vitro*, although the structural changes induced by mutants affect trafficking of the enzyme to the lysosome. Small molecule chaperones can be used to correct this trafficking defect. These compounds bind to the protein in the endoplasmic reticulum, accelerating the folding process and increasing their translocation to the lysosome, thereby reducing substrate accumulation. Several iminosugar inhibitors of GAA, such as duvoglustat, are known to chaperone the translocation of mutant GAA proteins. However, their impact on substrate reduction may be limited by their continued inhibition of the target enzyme, as well as limited selectivity towards GAA. We have previously reported an inhibitor (ML201) and through further work, we have now also identified the first non-inhibitory small molecule chaperone of acid alpha glucosidase, ML247. Here, we demonstrate that ML247 enhances mutant enzyme translocation using Pompe patient-derived fibroblasts. ML247 displays reasonable pharmacokinetics and might serve as a pivotal first step in efforts to develop a non-inhibitory molecular chaperone for the treatment of Pompe disease.

Probe Structure & Characteristics



CID/ ML	Target Name	IC ₅₀ /EC ₅₀ (nM) [SID, AID]	Anti-target Name(s)	IC ₅₀ /EC ₅₀ (μ M) [SID, AID]	Selectivity	Secondary Assay(s) Name: IC ₅₀ /EC ₅₀ (μ M) [SID, AID]
CID 44246403/ ML247	Acid α-Glucosidase	2818 [SID 85267344, AID 2110]	β-Glucosidase α-Galactosidase	>57 μM [AID 540341] >57 μM [AID 540361]	>10-fold	15 [SID 85267344, AID 602122]

Recommendations for Scientific Use of the Probe

Mutations in the lysosomal enzyme acid alpha-glucosidase (GAA) are the underlying cause of Pompe disease. Here, we present a small molecule chaperone that can correct the misfolding and mistrafficking of disease-causing mutant protein. All previously described small molecule chaperones of GAA are inhibitors of the enzyme. Here, we disclose a new class of non-inhibitory, selective small-molecule GAA chaperones that increase the translocation of several GAA mutants in primary patient fibroblasts without inhibiting the translocated protein's specific activity. These molecules increase the rate of hydrolysis in enzymatic assays, measured through

several of the classical fluorescent substrates of GAA. The probe molecule displays reasonable PK properties and exposure *in vivo* and is an ideal candidate for further characterization of its ability to reduce substrate accumulation *in vivo*. However, it should be noted that ML247 is not the most potent molecule with chaperone activity. With a potency of 160 nM, CID 44246394 may be more appropriate for *in vitro* studies, especially mechanism of action studies. Unfortunately, it is expected to be rapidly metabolized *in vivo*.



1 Introduction

Pompe disease, also called glycogen storage disease type II or acid maltase deficiency is an autosomal recessive disorder caused by the deficiency or dysfunction of the lysosomal enzyme acid alpha-glucosidase (GAA).¹ Epidemiological studies have estimated its frequency to be 1 in every 40,000 births.^{1,2} Functionally, GAA hydrolyzes terminal α -1,4 glucosidic linkages of glycogen in the lysosome. Mutations in this enzyme result in lysosomal enlargement due to glycogen accumulation, which is especially severe in cardiac and skeletal muscle, affecting breathing and mobility.¹ The only therapy currently approved by the FDA for Pompe Disease is enzyme replacement therapy (Myozyme), which is recombinant GAA produced in a Chinese hamster ovary cell line³. Although Myozyme has been proven to be clinically efficacious in children, the development of infusion-related reactions is common, and the majority of the patients (89%) test positive for IgG antibodies to acid alpha-glucosidase, reducing its clinical utility.⁴ In addition, some health plans have refused to subsidize Myozyme for adult patients, because it is only approved for children and has a high annual cost of treatment (\$300,000/year). Common observed adverse effects to Myozyme treatment are pneumonia, respiratory complications, infections, and fever. More serious reactions include heart and lung failure and allergic shock.⁵ These findings reinforce the need to develop new treatments for Pompe disease.

There are more than 100 different GAA mutations that can produce Pompe disease symptoms.⁶ Many of these mutant proteins retain their enzymatic activity *in vitro*, but they are not effectively transported to the lysosome. They start accumulating in the endoplasmic reticulum (ER), presumably due to their inability to fold properly or acquire the necessary shape to be targeted for transportation to the lysosome.⁷ Eventually, these mutants are tagged through ubiquitination and directed to the proteasome for degradation.

binding between substrate and inhibitor; therefore, weak inhibitors are preferred. In addition, their concentrations at the site of action also impact the equilibrium. For this reason, the dosing and schedule of these small molecule chaperones must be carefully tailored to achieve optimal exposures *in vivo* that favor enzyme translocation without reducing enzyme activity. All of these considerations make the development of iminosugar chaperones difficult; therefore, it is of interest to search for novel series of compounds with chaperone activity. In the past, our group has disclosed an alternative inhibitory series with GAA chaperone activity (Figure 1, ML201) with improved selectivity compared to the iminosugar inhibitors. Here, we describe the first *non*-inhibitory, selective small molecule chaperone of GAA, ML247.

2 Materials and Methods

The reagents and solvents were used as commercial anhydrous grade without further purification. The column chromatography was carried out over silica gel (100–200 mesh). ¹H NMR spectra were recorded with a Bruker 400 MHz spectrometer from solutions in CDCl₃ and DMSO-d₆. Chemical shifts in ¹H NMR spectra are reported in parts per million (ppm, δ) downfield from the internal standard Me₄Si (TMS, δ = 0 ppm). Molecular weight confirmation was performed using an Agilent Time-Of-Flight Mass Spectrometer (TOF, Agilent Technologies, Santa Clara, CA). A 3 minute gradient from 4 to 100% Acetonitrile (0.1% formic acid) in water (0.1% formic acid) was used with a 4 minute run time at a flow rate of 1 mL/min. A Zorbax SB-C18 column (3.5 micron, 2.1 x 30 mm) was used at a temperature of 50 °C. Confirmation of molecular formula was confirmed using electrospray ionization in the positive mode with the Agilent Masshunter software (version B.02).

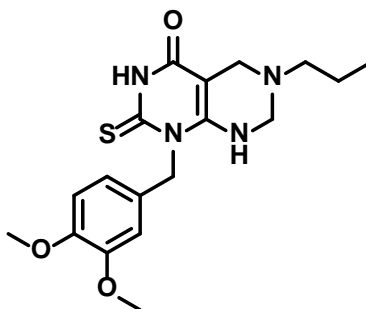
2.1 Assays

PubChem AID	Type	Target	Conc. Range	Samples Tested
2242	Primary qHTS	acid alpha-glucosidase	57.5 μ M – 0.7 nM	199,303
2112	Primary qHTS	acid alpha-glucosidase	57.5 μ M – 0.7 nM	236,748
2100	Primary qHTS	acid alpha-glucosidase	57.5 μ M – 0.7 nM	304,253
2101	Counterscreen	beta-glucosidase	57.5 μ M – 0.7 nM	326,770
1467	Counterscreen	alpha-galactosidase	57.5 μ M – 0.7 nM	229,459
2107	Counterscreen	alpha-galactosidase	57.5 μ M – 0.7 nM	239,498
2115	Confirmatory	acid alpha-glucosidase	287 μ M – .001 μ M	296
2113	Confirmatory	acid alpha-glucosidase	287 μ M – 0.001 μ M	296
2110	Secondary	acid alpha-glucosidase	282 μ M – 0.001 μ M	70
2111	Secondary	acid alpha-glucosidase	282 μ M – 0.001 μ M	59
2108	Counterscreen	alpha-galactosidase	287 μ M – 0.001 μ M	296
2109	Counterscreen	alpha-galactosidase	287 μ M – 0.001 μ M	296
2293	Secondary	acid alpha-glucosidase	10 μ M – 0.1 μ M	1
602122	Secondary	acid alpha-glucosidase	15 μ M	2
1473	Summary	acid alpha-glucosidase	N/A	N/A

Table 1. List of all assays screened.

Detailed descriptions and protocols of all these assays listed in Table 1 can be found in the appendix. For further information, including data, please see <http://pubchem.ncbi.nlm.nih.gov/>, especially the summary assay for the project, AID 1473. Curves can be viewed by looking at the data and selecting the graph function in “outcome”.

2.2 Probe Chemical Characterization



Probe Characterization of ML247

*Purity >95% as determined by LC/MS and ¹H NMR analyses.

1-(3,4-dimethoxybenzyl)-6-propyl-2-thioxo-2,3,5,6,7,8-hexahydropyrimido[4,5-d]pyrimidin-4(1H)-one. ¹H NMR (400MHz,DMSO-*d*₆) δ 12.08 (s, 1H), 7.20 (s, 1H), 6.88 (d, *J* = 4.4 Hz, 2H), 6.65 (d, *J* = 8.0 Hz, 1H), 5.51 (br s, 2H), 3.92 (s, 2H), 3.70 (s, 6H), 3.39 (s, 2H), 2.32 (t, *J* = 7.2 Hz, 2H), 1.43 (q, *J* = 7.2 Hz, 2H), 0.84 (t, *J* = 7.2 Hz, 3H); HRMS (ESI) *m/z* calculated for [C₁₈H₂₄N₄O₃S + H]⁺ 376.1569, found 376.1573.

Internal ID	MLS ID	SID	CID	ML	Type	Source
NCGC00183885-01	MLS002699808	85267344	44246403	ML247	Probe	NCGC
NCGC00182856-01	MLS000729403	85267296	1512045		Analog	NCGC
NCGC00183621-01	MLS002699809	85267337	44246396		Analog	NCGC
NCGC00183442-01	MLS002699810	85267314	44246374		Analog	NCGC
NCGC00183589-01	MLS002699811	85267334	44246394		Analog	NCGC
NCGC00182855-01	MLS002699812	85267104	1259573		Analog	NCGC

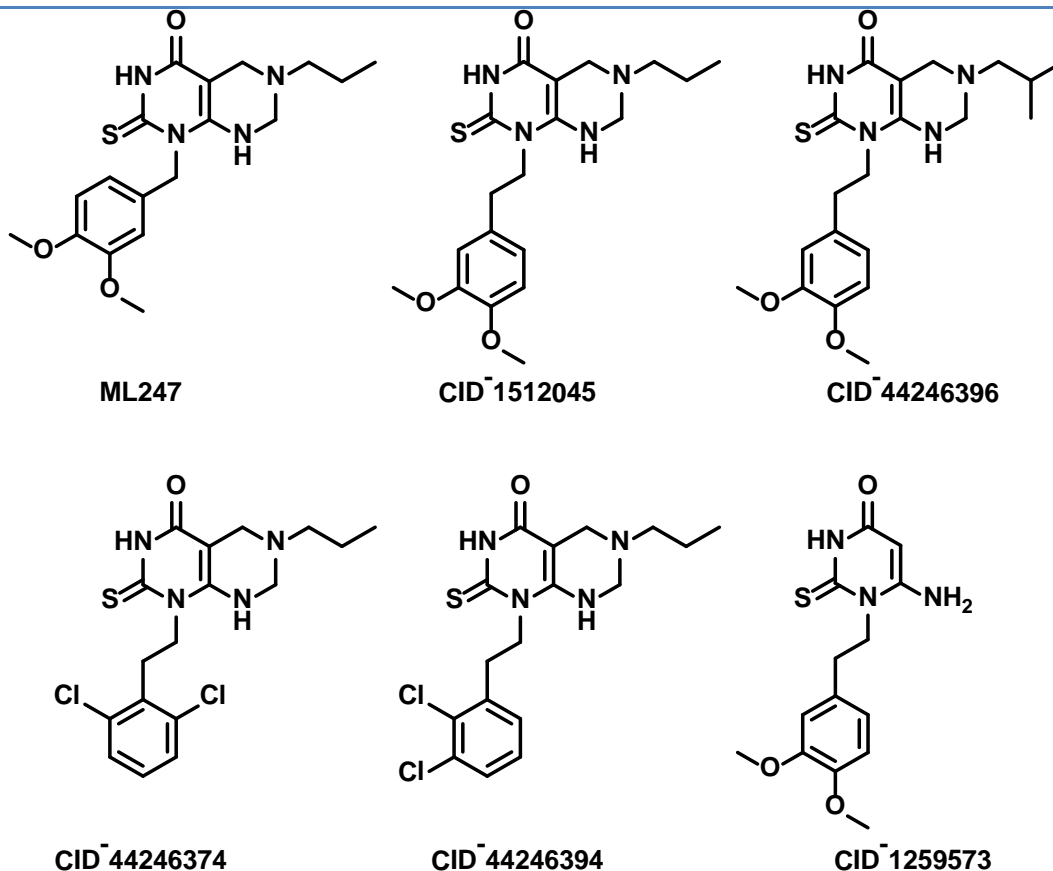


Figure 2. List and structure of probe and analogs that have been submitted to the MLSMR.

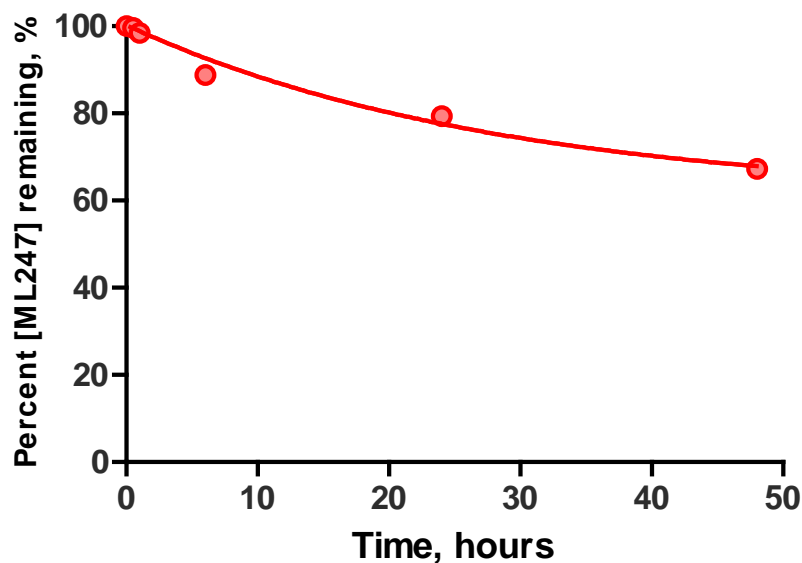
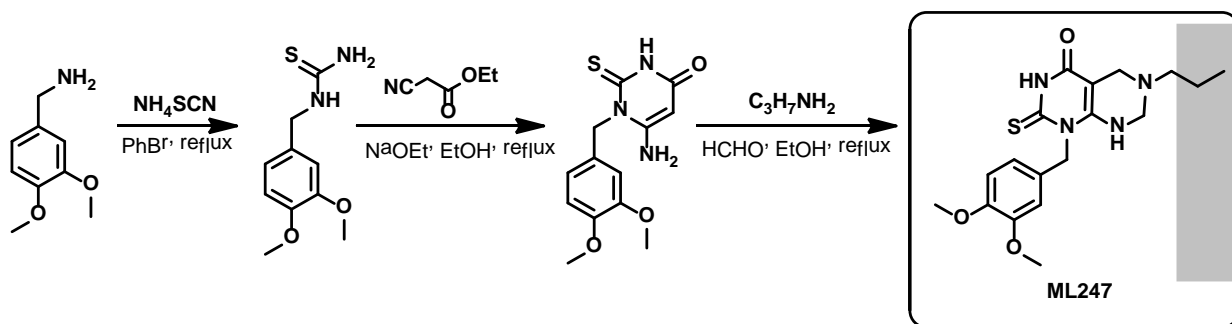


Figure 3. Stability of ML247 in DPBS (pH 7.4) at room temperature over 48 hours.

2.3 Probe Preparation



Scheme 1. Synthetic route to ML247.

Scheme 1 shows the synthetic route used to ML247. Ammonium thiocyanate (27.58 mmol) was added to a stirred solution of the 3,4-dimethoxybenzyl amine, shown on the left (27.58 mmol) in bromobenzene (10 mL) at room temperature. The reaction mixture was heated at reflux temperature for 6 h. The reaction mixture was cooled to room temperature and concentrated under reduced pressure. The crude residue was purified by column chromatography (2–10% MeOH in CH_2Cl_2) to produce the corresponding thiourea above. The products were characterized by MS analysis and subjected to the next step without further purification; yield = 33%, MS (ESI) m/z $[\text{M} + \text{H}]^+$ of 241 observed.

The thiourea (2.08 mmol) and ethyl cyanoacetate (2.28 mmol) were then added to a solution of sodium (2.08 mmol) in ethanol (5 mL). The reaction mixture was heated at reflux for 4 h. The reaction mixture was cooled to room temperature and concentrated under reduced pressure. The crude residue was purified by column chromatography (1–3% MeOH in CH₂Cl₂) to afford the pyrimidinone shown above. The products were characterized by ¹H NMR and MS analysis.

Yield = 31%; ¹H NMR (400 MHz, DMSO-*d*₆) δ 11.86 (s, 1H), 7.06 (s, 2H), 6.97 (s, 1H), 6.88–6.82 (m, 2H), 4.85 (s, 1H), 4.48 (br s, 2H), 3.73 (s, 3H), 3.70 (s, 3H), 2.84 (t, *J* = 8 Hz, 2H); HRMS (ESI) *m/z* calculated for [C₁₄H₁₇N₃O₃S + H]⁺ 307.0991, found 307.0993.

n-Propylamine (4.55 mmol) and formaldehyde (6.50 mmol) were added to a solution of the product amine from the previous step (3.25 mmol) in ethanol (20 mL). The reaction mixture was heated at reflux for 3 h, cooled to room temperature, and filtered through a sintered glass funnel to afford the final product, with a yield of 24%. The compound was characterized by ¹H NMR and MS analysis, and HRMS.

3 Results

3.1 Summary of Screening Results

Initially, an enzyme assay was developed using recombinant GAA and a pro-fluorescent substrate, 4-methylumbelliferyl- α -D-glucopyranoside (4MU- α -Gluc). Upon hydrolysis by GAA, this substrate forms two products, glucose and 4-methylumbelliferone (4MU). 4MU emits fluorescent signal at 440 nm when excited at 365 nm. This is a simple and homogenous assay that is suitable for HTS and can theoretically detect both activators and inhibitors. Using this assay, 199,176 compounds were tested (AID 2242). Signal to background ratios averaged 20-fold and plate Z's averaged 0.7, indicating a robust assay. A counterscreen was run using recombinant alpha-galactosidase (GLA) and a similar pro-fluorescent 4MU-based substrate (AID 1467). Fluorescent compounds will appear to be enzyme activators in both assays, and by looking for selective activators of GAA, we hoped to identify non-inhibitory chaperones. We were not able to confirm any of the compounds from this initial screen as GAA activators.

Due to concerns that the recombinant, purified assay might be missing important protein factors, and the previous difficulty in finding compounds active in cell-based assays using hits against

other purified lysosomal targets, the primary screen was reformatted to measure alpha-glucosidase specific activity from spleen homogenate. Signal to background ratios averaged 40-fold, and the average plate Z' from the screen was 0.8 (Figure 4). By then, the MLSMR collection had grown, and 232,184 compounds were screened (AID 2112). The hit, CID 1512045, was cherry-picked from the MLSMR for confirmation based on selectivity against GLA in a similar screening format (AID 2107); this compound was not screened in the original primary screen and was the only compound whose activity was confirmed. The compound was then ordered from a commercial vendor and later re-synthesized in-house. This compound activates GAA in both the purified acid alpha-glucosidase assay and the tissue homogenate assay, with similar activity in both (Figure 5). CID 1512045 was not auto-fluorescent by spectral profiling and did not show activity against the related enzymes alpha-galactosidase and beta-glucosidase (glucocerebrosidase). Structure-activity relationship studies were then undertaken, leading to the identification of the probe compound, ML247.

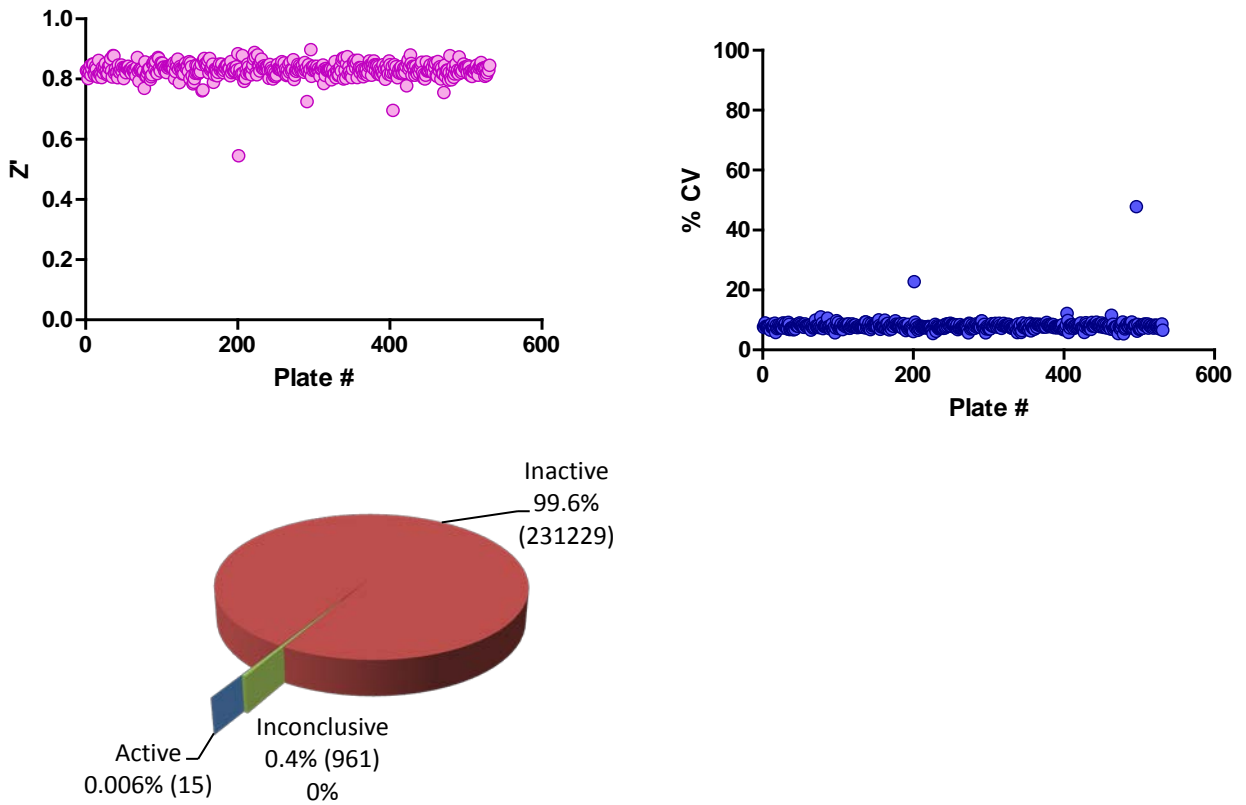
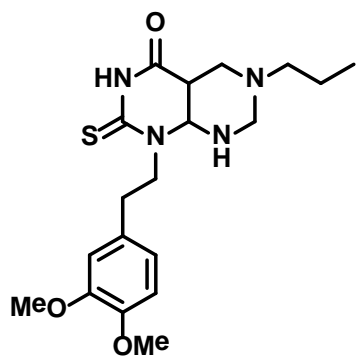


Figure 4. Performance of primary qHTS screen. Both Z' and %CV are very stable and consistent, indicating a robust screen. The pie chart depicts distribution of activity.



CID⁻1512045 (1)

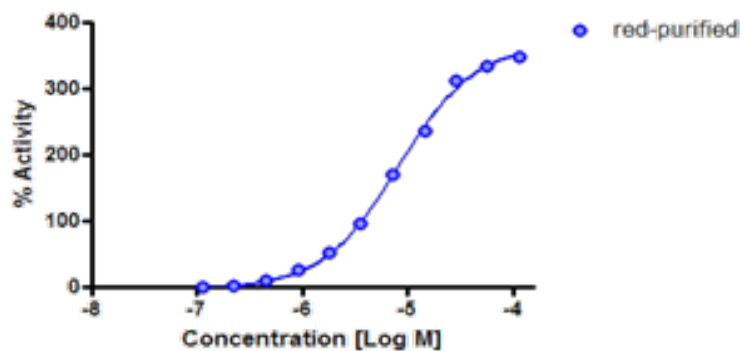
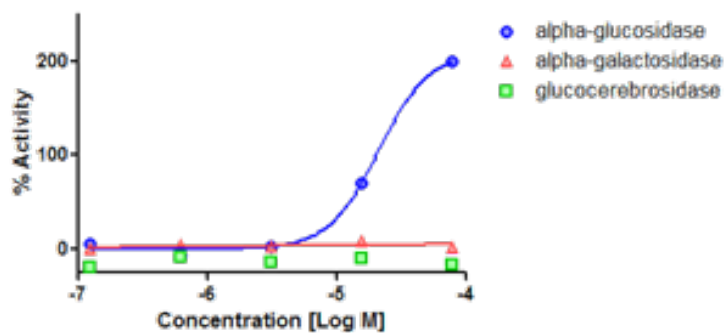


Figure 5. The hit CID 1512045 (1) was inactive in the counterscreens and had an AC₅₀ of 14.1 μ M in the primary screen. The counterscreens were performed using 4MU substrate and the purified enzyme. Confirmation of the hit was carried out by using the resorufin substrate with the purified enzyme.

3.2 Dose-Response Curves for Probe

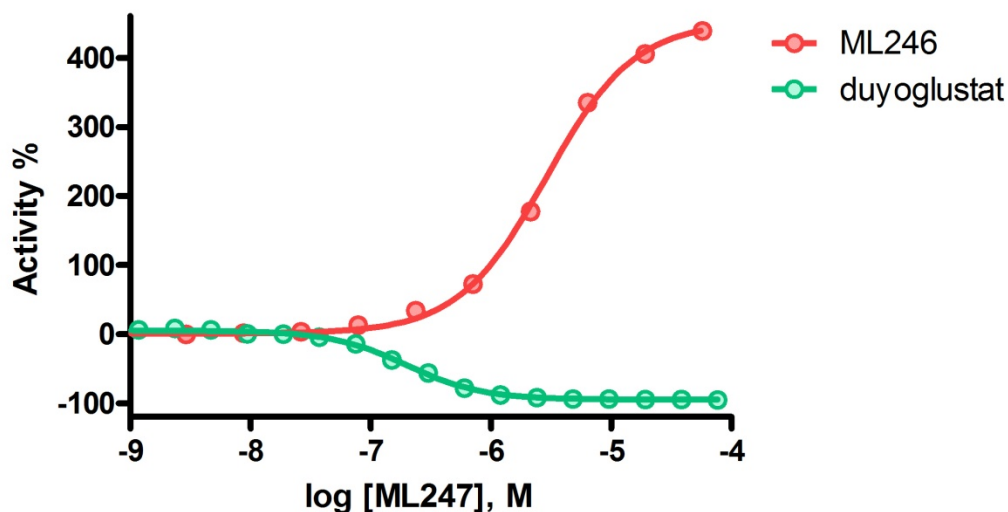


Figure 6. Dose response curve for probe ML247 (*red*) and the inhibitor CID 176077 (duvoglustat, *green*) in the alpha-glucosidase assay using purified enzyme against the resorufin tagged substrate.

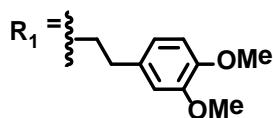
3.3 Scaffold/Moiety Chemical Liabilities

It is not expected that this scaffold has any functional groups with serious chemical liabilities. Based on the results of microsomal stability studies (section 3.5), the probe has excellent stability in biological media. However, it is noteworthy that in the 48 hour compound stability study in PBS buffer, stability was below 75% (Figure 3). We were unable to determine whether the compound was slowly precipitating from solution or if there was hydrolysis of the thiourea moiety under the conditions tested. If use requires extended incubation times in aqueous media, compound stability should be closely monitored.

3.4 SAR Tables

For many compounds less active than the original hit, we were unable able to observe an inflection in the concentration-response at higher compound concentrations, and so we were unable to estimate an AC_{50} for those compounds. Furthermore, it was not possible to evaluate activity at higher than 100 μ M due to solubility limitations of the compounds in DMSO. Instead, SAR was evaluated on the basis of a combination of AC_{50} s and the maximum efficacy reached

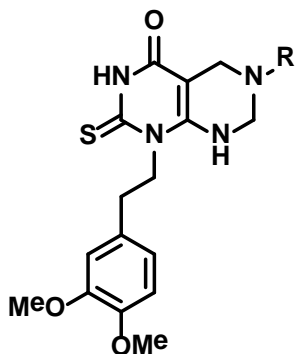
with each compound at 77 μ M. That is the data reported below. Full concentration-response curves for every compound can be found in PubChem.



Entry	Internal ID	SID	CID	Core structure	Activity [μ M] (Efficacy [%])
1	NCGC00182856-01	85267296	1512045		2'0 (365)
2	NCGC00183886-01	85267345	44246404		14'1 (297)
3	NCGC00054598-01	4257056	1259573		Inactive
4	NCGC00183587-01	85267332	44246392		Inactive
5	NCGC00183884-01	85267343	44246402		Inactive
6	NCGC00183622-01	85267338	44246397		Inactive
7	NCGC00183888-01	85267347	44246406		Inactive

Table 2. Analogs with modifications at the core template. Activity is reported as the micromolar potency of the compound (where available) and the efficacy of the compound at 77 μ M, the highest concentration tested. Efficacy is the absolute increase in substrate turnover as a percentage. Where the activity is listed as inactive, the compound

activity at 77 μM was not statistically significant. Additional core modifications that were also inactive are not shown, but available in PubChem.



Entry	Internal ID	SID	CID	R	Activity [μM] (Efficacy [%])
8	NCGC00182856-01	85267296	1512045		2.0 (356)
9	NCGC00183516-01	85267327	44246387		7.9 (282)
10	NCGC00183515-01	85267326	44246396		0.6 (338)
11	NCGC00183621-01	85267337	44246396		11.2 (233)
12	NCGC00183517-01	85267328	44246388		1.8 (334)
13	NCGC00183590-01	85267335	17271141		7.9 (274)

Table 3. SAR table with further modifications to the core's alkyl substituent. Activity is reported as in Table 2.



Entry	Internal ID	SID	CID	R ₁	Activity [μ M] (Efficacy [%])
14	NCGC00183458-01	85267320	44246380		N/A (31)
15	NCGC00183624-01	85267340	44246399		N/A (192)
16 ML247	NCGC00183885-01	85267344	44246403		2.8 (365)
17	MLS000729355-02	85267113	1511383		N/A (142)
18	NCGC00183589-01	85267334	44246394		0.16 (346)
19	NCGC00183442-01	85267314	44246374		1.1 (332)
20	NCGC00183459-01	85267321	44246381		N/A (166)
21	NCGC00183460-01	85267322	85267322		Inactive
22	NCGC00183514-01	85267325	44246385		Inactive
23	NCGC00183461-01	85267323	44246383		Inactive

Table 4. SAR table with modifications to R₁ of the molecule. Activity is reported as in Table 2.

Tables 2-4 show the SAR of select compounds; the full set of analogs can be found in PubChem. SAR changes show that all core modifications that were synthesized (Table 2) failed to further activate hydrolysis of our fluorogenic substrate, and even replacement of the thiocarbonyl functional group by a carbonyl group diminished activity. Replacement of the pendant aromatic ring at position 1 with various alkyl chains also abolished activity. Several heteroaromatic rings pendant to position 1 were poorly active or greatly reduced the activity of the lead compound. Shortening the linker from two carbons to one, **16**, is well tolerated and produces a small increment in efficacy. Optimization of the substitution pattern for the phenethyl group at position 1 (**18**) showed that electron donating di-substituted compounds tend to provide better efficacy. In addition, it can be seen that the most active molecules have very reasonable calculated log P and tPSA, and in general, increments of log P and reduction of tPSA correlated with improvements in activity. None of the compounds tested activate the hydrolysis of substrates for other glycosidase enzymes, such as alpha-Galactosidase A or Glucocerebrosidase (data not shown). Overall, the data shows a narrow SAR in which most modifications to the core of the molecule yielded diminished activation of hydrolysis. Full concentration-response curves for the most potent compounds **1**, **10**, **16**, **18**, **19** are shown in Figure 7. The best compound, **18**, had an AC₅₀ of 0.16 μM, and the probe molecule, ML247 (**16**), had a potency of 2.81 μM in this assay. We characterized *in vitro* activity against GAA, and then we proceeded to characterize the capacity of the most active compounds to translocate GAA to the lysosome in patient-derived fibroblasts as *prima facie* evidence of their capacity to chaperone GAA.

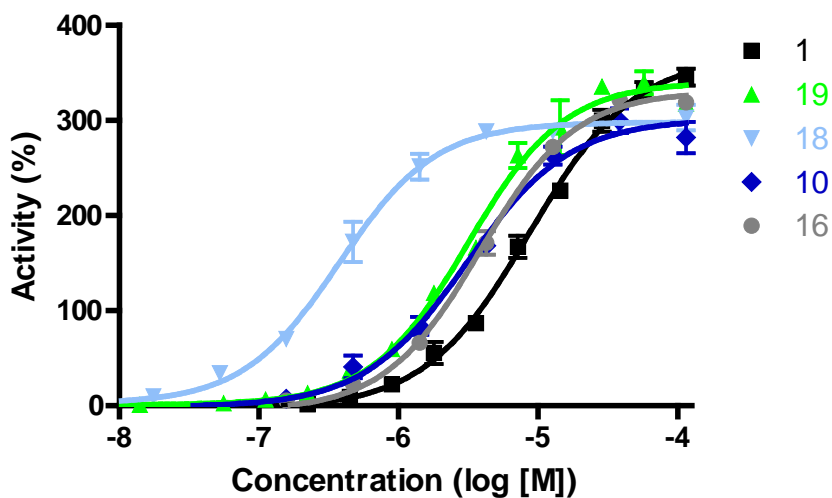


Figure 7. Full concentration-response profiles of the best activators in the resorufin substrate and purified enzyme assay.

3.5 Cellular Activity

Chaperone Activity in Pompe Patient-derived Fibroblasts

To measure the capacity of our compounds to activate ER-lysosome translocation of GAA, we treated Pompe patient-derived fibroblasts with compound for five days, followed by immunostaining (GAA and Cathepsin D as lysosomal marker), wash, and image analysis.¹³⁻¹⁴

Pompe fibroblasts are difficult to obtain, and in general, they grow slowly; they can only be expanded by a few passages. Two cell cultures derived from a single patient with the mutations p.Y455C/p.G638W were obtained. The residual specific activity of these patient-derived fibroblasts is around 3% of the activity displayed by fibroblast with wildtype GAA (data not shown).

Although the specific activity of GAA in fibroblasts (skin biopsies) is definitive for a Pompe disease diagnosis, fibroblasts do not express GAA in abundant amounts, and that expression decreases with increasing passage number, even for wildtype cells. Nevertheless, the present patient-derived cells had sufficient protein expression to enable us to characterize the chaperone activity of this series, which is done by examining the co-localization of GAA staining with lysosome marker staining (CathD). No lysosomal GAA staining can be seen in DMOS vehicle-

treated Pompe cells. As a reference, in our hands, the GAA signal in wildtype fibroblast by passage 8 could be observed by staining in 10% of the cells.

The inhibitory chaperone duvoglustat is a non-selective iminosugar currently in clinical trials for Pompe disease. The chaperone activity of duvoglustat varies by mutation, and there is no previous literature indicating whether duvoglustat is active against p.Y455C/p.G638W GAA mutations. No chaperone activity was observed at compound concentrations of 1, 5, and 15 μM (data not shown). At 20 μM , translocation of GAA to the lysosome occurred in 3% of the cells. These values are in the same range as those reported for other GAA mutants, where duvoglustat increased GAA translocation at 20 μM . Duvoglustat does not increase the translocation of wildtype GAA (data not shown).

The initial hit compound **1** increases translocation of GAA to lysosomes in patient-derived fibroblasts. However, compound **16** gave the most robust responses, with around 10% translocation of mutant GAA to the lysosomes at 20 μM . Translocation could still be observed at 15 and 10 μM , but not at 5 μM . Comparison between the results obtained with duvoglustat and with compound **16**, and the probe molecule ML247, show that at the same concentration, the probe molecule is superior (Figure 8).

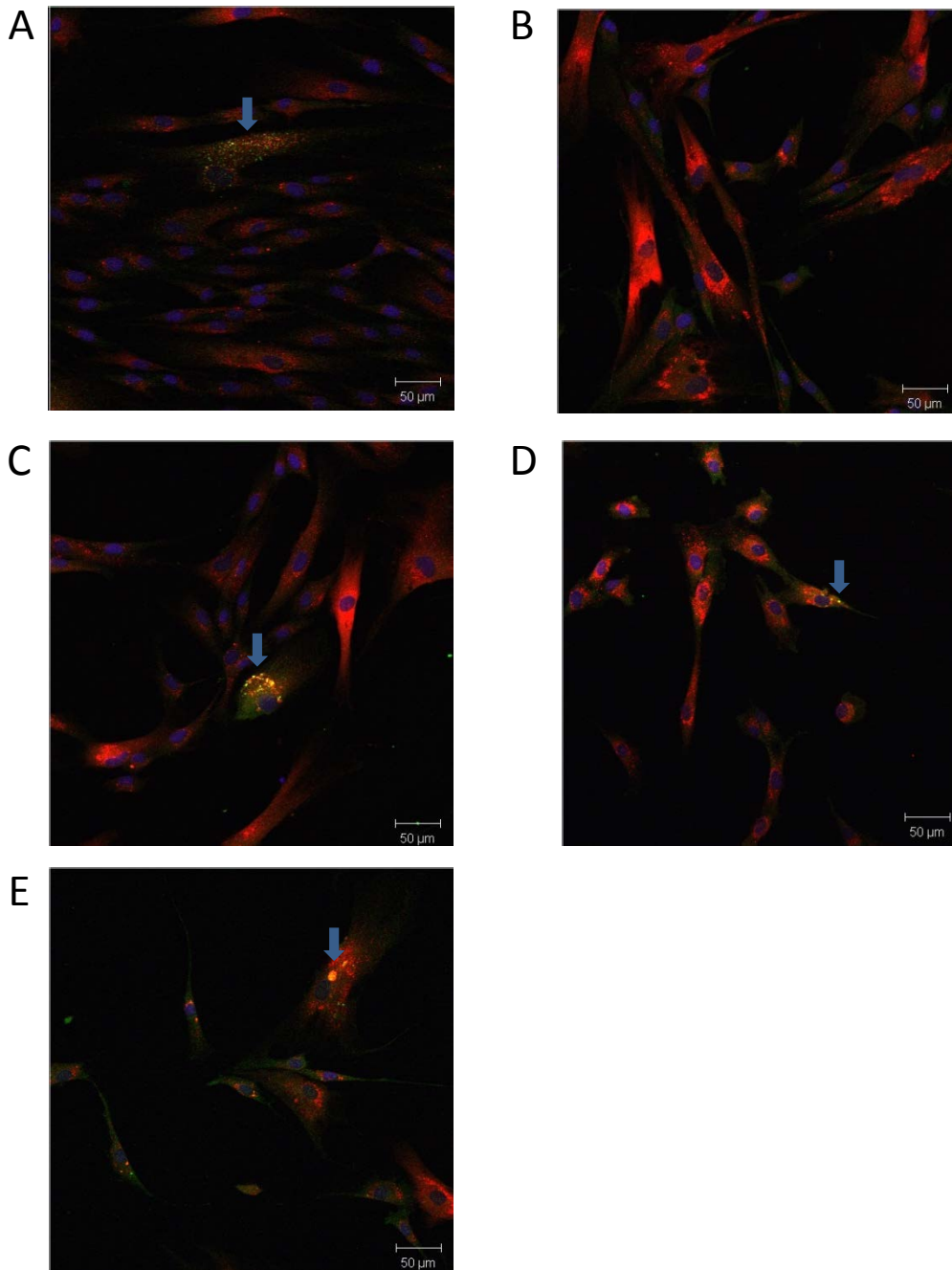


Figure 8. Probe compound **ML247** restores GAA translocation to the lysosome (blue arrows). False-colored images of fibroblast cells show DAPI nuclear stain (blue), the lysosomal marker Cathepsin D (red) and GAA (green) in cells from (A) an unaffected donor with wildtype GAA, and (B-E) Pompe patient-derived cells with p.Y455C/p.G638W mutations. Cells were cultured for five days with compound that was dispensed using a DMSO vehicle. Yellow color (overlapping green and red) indicates co-localized lysosomal GAA protein, typically present in (A) DMSO vehicle treated wildtype cells, but absent in (B) DMSO vehicle treated patient-derived cells, and

partially restored with (C) 20 μM duvoglustat, (D) 15 μM compound **1**, and more strongly with (E) 15 μM compound **16**.

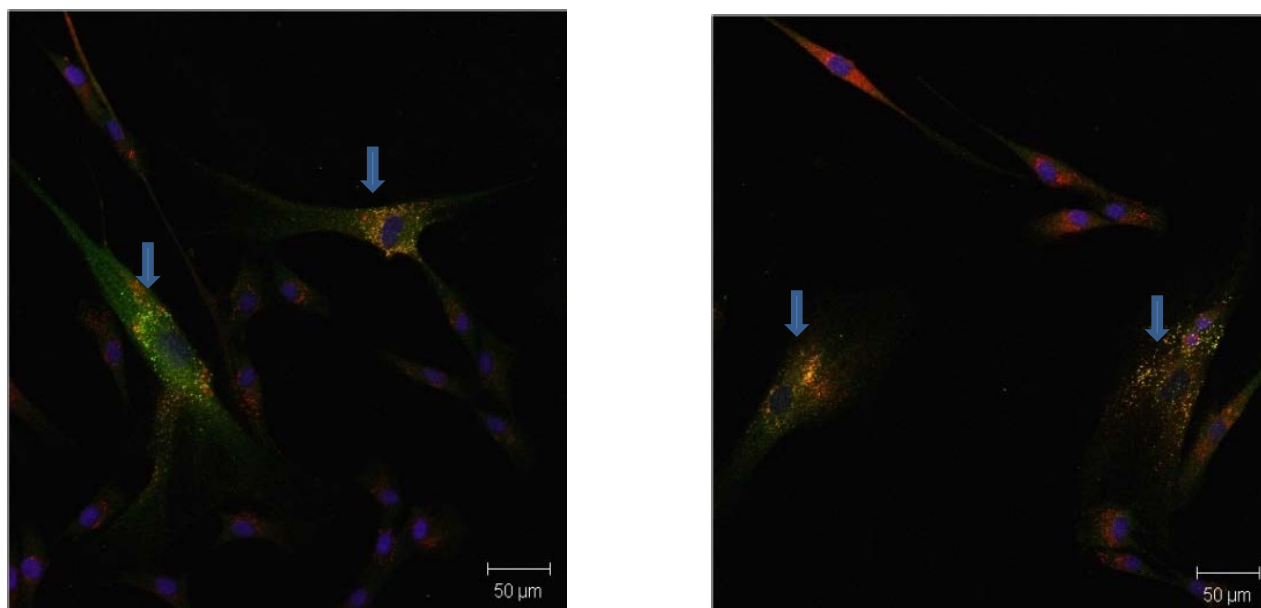


Figure 9. Two representative fields showing profound restoration of lysosomal GAA in patient-derived fibroblasts (blue arrows), upon five day incubation with 20 μM probe compound ML247. Coloring scheme is the same as Figure 8.

3.6 Profiling Assays

Ultimately, compounds from this series need to be evaluated *in vivo* to demonstrate their therapeutic potential. The probe molecule from the series was selected for its potential to demonstrate activity in that setting; this depended not only on potency *in vitro*, but also activity in the cell-based translocation assay, microsomal stability, and to a lesser extent, Caco-2 permeability (Table 5). The probe compound, ML247, has excellent Caco-2 permeability ($> 5\text{cm}^{-8}/\text{s}$) and robust stability, with $>60\%$ remaining after a 60 minute incubation with mouse liver microsomes. The addition of NADPH also had little effect on compound stability, indicating only very modest P450 mediated metabolism. In contrast, compounds **1**, **18** and others (not shown) suffer from significant P450-mediated metabolism. Based on these results, the probe molecule, compound **16**, was further studied in a single-dose pharmacokinetics experiment. At 50 mg/kg IP dosing, no acute toxicity was observed (Figure 10). Compound half-life was 2.75 hours in plasma, with concentrations in plasma, liver and heart all exceeding 10 μM at one hour.

Reasonable exposure was generated by the compound to warrant exploratory testing in an *in vivo* efficacy model.

Compound	Aqueous Kinetic Solubility	Mouse liver microsomal stability (% remaining after 60 min)		Caco-2 ($10^{-6} \text{ cm s}^{-1}$)		Efflux Ratio
	μM	No NADPH	NADPH	A to B	B to A	
ML247 (16)	288.8	100.62	63.18	5.3	28.9	5.4
CID 44246394 (18)	N/A	104.59	2.06	27.5	50.4	1.8
CID 1512045 (1)	N/A	4.32	4.32	2.3	31.4	13.4

Table 5. *In vitro* profile of ML247.

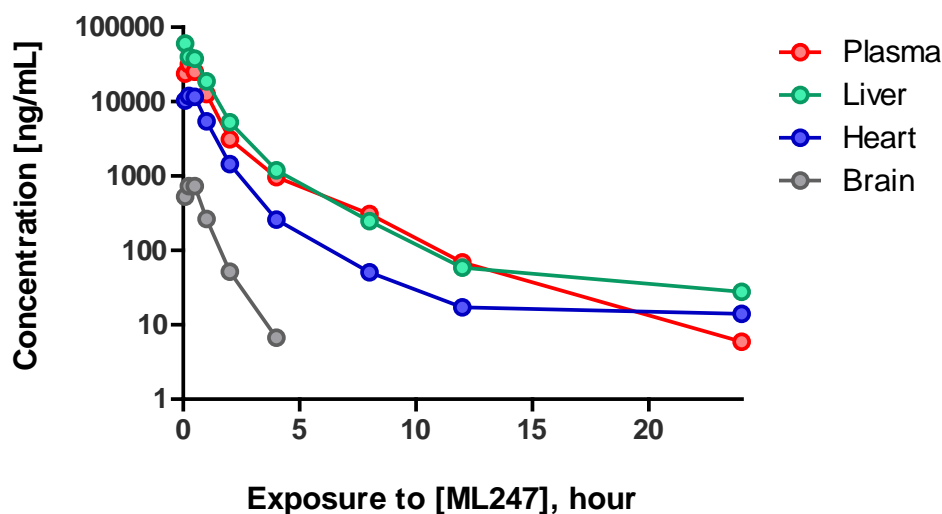


Figure 10. *In vivo* exposure by ML247 following a single 50 mg/kg IP dose in mice. Further information can be found in the appendix.

4 Discussion

The ability of a small molecule to act as a protein chaperone that enhances protein translocation is normally measured using cell imaging assays. These assays are based on the immunostaining of a lysosomal hydrolase with specific antibodies and a lysosomal marker, such as LAMP2. These cell imaging assays are complicated and very labor intensive. They typically require at least five days of exposure to the chaperone compound, fixation of cells, treatment with antibodies, multiple wash steps, and finally high-content fluorescent imaging detection; they are

not amenable to high throughput screening (HTS) and are unsuitable for supporting structure-activity relationship (SAR) studies. Thus, as a surrogate assay that is amenable to HTS, researchers in the field rely on enzymatic hydrolysis assays as the primary screening method to identify potential chaperones. Theoretically, this approach can identify activators and inhibitors of lysosomal hydrolases from a large compound library. Then, the chaperone activities of compounds are validated using the immunostaining assay.

The aim of this project was to identify non-inhibitory small molecule chaperones of GAA for the study and potential treatment of Pompe disease. These types of molecules have never been disclosed in literature, and from a therapeutic point of view, would be more desirable than the iminosugar chaperones currently in clinical trials. Non-inhibitory chaperones are allosteric binders by definition, because it is impossible to increase the rate of hydrolysis by competing at the active site with substrate, and should be more selective against other glycosidases, also possessing a wider therapeutic window than current treatments. We hypothesized that the present lack of such compounds was directly related to the screening methodology employed. Until now, the assays that have been used to measure enzyme modulation employed detergents to non-physiologically activate the enzyme. In retrospect, it may be the case that the optimization of the assay for obtaining maximal signal in these conditions might over-activate the enzyme into a conformation different than its physiological state, preventing the finding of activators. It has also been previously demonstrated that many glycosidases require allosteric activation by co-factors to be functional.¹² We suggest the use of tissue homogenate preparations as the preferred approach to measure the functional activity of lysosomal enzymes. These preparations contain all of the necessary co-factors for enzyme activation in the natural environment, and as we demonstrate in our screening strategy, allow for the discovery of activating compounds.

The ability of an inhibitor to modulate the enzyme's activity does not always correlate with its ability to induce and accelerate the folding and translocation of mutant enzyme. Therefore, inhibitors and activators can exist without chaperone activity, and vice-versa. If a particular compound series has both the capacity to modulate the activity of the enzyme and the ability to enhance its translocation, then compounds with a greater potency in modulating the enzymatic activity also usually show better translocation properties. In these cases, lower AC₅₀ values

imply higher affinity toward the enzyme, which should correlate with a greater capacity to induce a folded conformation and better translocation ability. However, even within a family of modulators, it is possible to increase the binding affinity of the series for the enzyme without incrementing its inhibitory or activatory activity; therefore, the best chaperone molecules within a series do not necessarily have to be the most potent modulators. Importantly, within series having modulatory and chaperone properties, the modulation of the enzyme activity can be used as an indirect method for measuring increments in affinity toward the enzyme, and therefore for improving the chaperone capacity of the series. From a therapeutic point of view, an ideal chaperone series should increase the translocation of the protein without inhibiting its enzymatic function.

It is also important to point out that from a structural point of view, lysosomal hydrolyses adopt slightly different conformations when accommodating different substrates in their active sites. Thus, the conformation that GAA adopts during the hydrolysis of the natural polymeric substrate glycogen could be substantially different than the one adopted for the hydrolysis of 4-methylumbelliferyl α -D-glucopyranoside or resorufin α -D-glucopyranoside. Allosteric small molecule chaperones able to bind with the enzyme and promote a particular conformation might influence the hydrolytic reaction of different substrates differently, depending on the substrates used. For this reason, activators of the hydrolysis of 4-methylumbelliferyl α -D-glucopyranoside do not necessarily have the same potency when they are evaluated using resorufin α -D-glucopyranoside or glycogen. The most relevant hydrolytic reaction can then be used for SAR studies to identify compounds with increased affinity toward the enzyme for testing in the chaperone assay.

After analyzing the expression of GAA from several different tissues, we decided to use human spleen homogenate as the source of the enzyme preparation, because of its high GAA specific activity. In contrast to other LSDs, there is not one dominant genotype in Pompe disease; therefore, we completed the primary screening using wildtype GAA. Only one series of activating molecules was confirmed. Additional LC/MS studies (Figure 11) showed that the activation of 4MU- α -glu hydrolysis was real and not a fluorescent artifact. Later studies with our hit (**1**), ML247, and other analogs showed that this series was selective toward modulating the activity of GAA. The capacity of this series to activate the hydrolysis of 4MU- α -glu did not

reproduce upon the use of natural substrate glycogen (data not shown), but that measurement was carried out using an isolated enzyme preparation, because the reaction cannot be evaluated in tissue homogenate due to the high background of the product of the reaction (glucose) in that setting. Importantly, our molecules never displayed inhibitory activity in any of the enzymatic assays and conditions evaluated. In addition, we also showed that our probe molecule was able to increase the translocation of wildtype and mutant GAA to the lysosome. For the specific mutation used for this evaluation using Pompe fibroblasts, our probe molecule, ML247, displayed better translocation capacity (10% of the cells vs 3% for duvoglustat) than the known inhibitory chaperone duvoglustat, currently in phase II clinical trials.

Finally, SAR changes show that all core modifications that were synthesized (Table 2) failed to further activate hydrolysis of our fluorogenic substrate, and even replacement of the thiocarbonyl functional group by a carbonyl group diminished activity. The SAR data also showed a low tolerance for most modifications, but we did manage to improve the AC_{50} 16-fold of our lead compound (section 3.3 SAR). In addition, it can be seen that the most active molecules have very reasonable calculated log P and tPSA, and in general, increments of log P and reduction of tPSA correlated with improvements in activity. Moreover, microsomal stability and Caco-2 permeability studies prompted us to carry out *in vivo* pharmacokinetic evaluation (3.5 Profiling Assays). We observed that our probe molecule displayed reasonable levels and exposure in relevant tissues for the disease (heart, liver), and warrants further study of its efficacy.

In conclusion, we present for the first time a non-inhibitory chaperone series with capacity to translocate GAA mutants with improved activity in regards to the current clinical trial compound duvoglustat. Pharmacokinetic properties and therapeutic window considerations place our probe molecule as an excellent candidate for further advancement studies toward the treatment of Pompe disease.

4.1 Comparison to existing art and how the new probe is an improvement

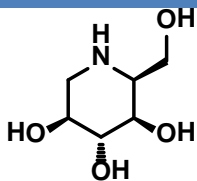
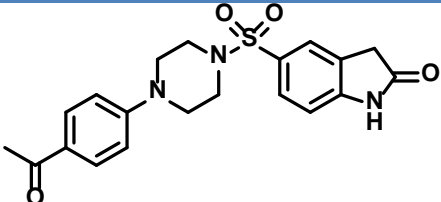
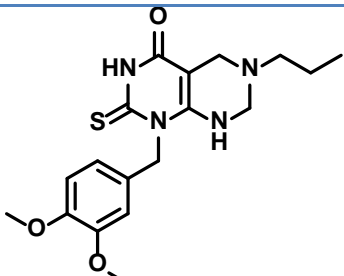
Name	Structure	Hydrolysis	Translocation
duvoglustat		Inhibitory	Modest effect observed at 20 μ M
ML201		Inhibitory	Not tested
ML247		Non-inhibitory	Robust effect observed at 15 μ M

Table 6. Comparison of ML247 to prior art.

All of the small molecule chaperones reported in the literature are enzyme inhibitors, with the majority being iminosugars. One of these, duvoglustat, is currently being tested in a phase II clinical trial as a pharmacological chaperone for Pompe disease by Amicus Therapeutics Inc.⁹ Iminosugars bind at the active site of the enzyme, mimicking the transition state of the glycolytic reaction. Binding of iminosugars to the active site stabilizes the protein in an active conformation and facilitates its transport to the lysosome. Although the ability of iminosugars to act as protein chaperones has been well established, this strategy has several pitfalls. First, because of their mode of action as substrate mimetics, iminosugars tend to be poorly selective⁸, inhibiting several glycosidases simultaneously and producing many side effects. Second, patient responses have also been highly variable, due to population differences in the expression of membrane transporters, which affect how the iminosugars are actively transported through the gastrointestinal track and the blood-brain-barrier. Lastly and most importantly, due to their intrinsic inhibitory activity, the therapeutic window of these molecules can be small because of the narrow difference in concentration at which they are translocation inducers and inhibitors.^{8,10}

4.2 Mechanism of Action Studies

To be sure that these compounds increase the hydrolytic rate of 4MU- α -glu, and do not interfere with the assay readout, we decided to follow the reaction directly using LC/MS with the initial hit, **1**. Figure 11 shows how the product of the reaction increased when we incremented the concentration of compound **1**. No 4MU product was produced with compound in absence of enzyme (data not shown).

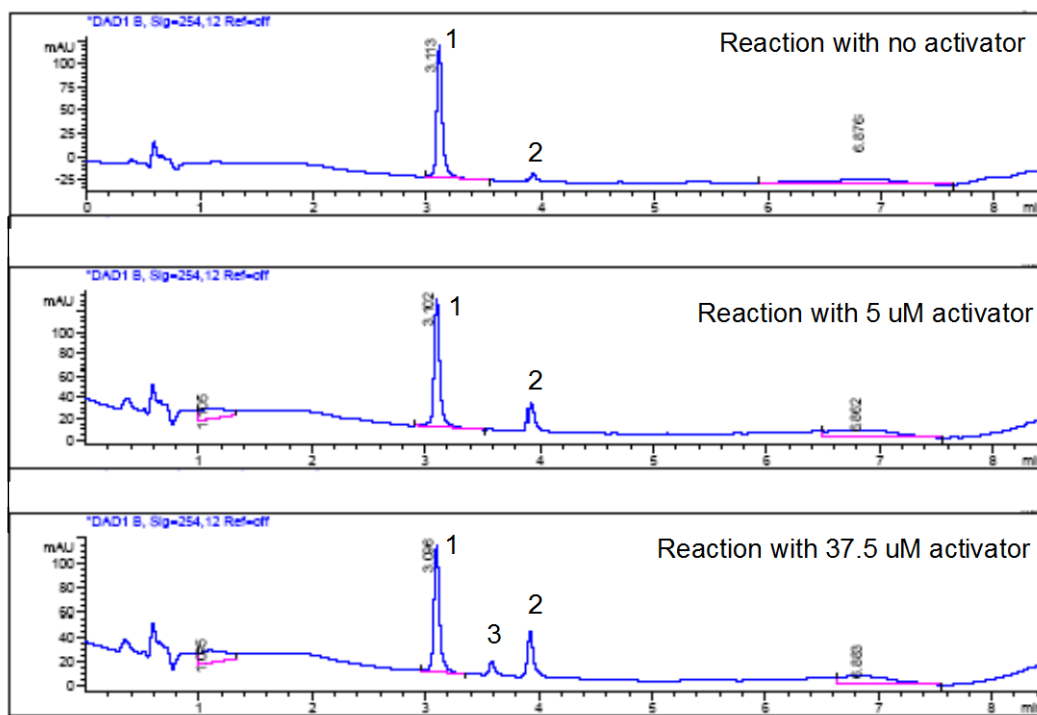


Figure 11. LC/MS blue dye hydrolysis evaluation. Liquid chromatography traces of reaction mixtures shown. Peak identity assigned by mass spectrometry. Peak 1: 4MU- α -glu, peak 2: 4MU, peak 3: hit compound **1**.

4.3 Planned Future Studies

As illustrated in our translocation studies, several of our best compounds, including our probe molecule ML247, are currently able to increase the trafficking of GAA between the ER and the lysosome (Figure 9). ML247 is not an inhibitor, displaying good pharmacokinetics with proper distribution and very reasonable exposure. We believe that this molecule is a good candidate for further studies in Pompe disease. Unfortunately, at present, there are no commercial point mutant mouse models of Pompe disease where chaperone molecules can be evaluated *in vivo*. Nevertheless, Amicus Pharmaceuticals has been able to advance an iminosugar inhibitor

chaperone to phase II clinical trials using their proprietary approach. Another direction to pursue is testing the effect on compound treatment on wildtype animals, because the probe molecule is able to increase the translocation of wildtype GAA. We hope that the compound might generate a measurable increase in specific activity in disease-related tissues, allowing us to evaluate the therapeutic value of this molecule. We have also published our results¹⁵ and hope that our findings will be of interest to the community at large and will lead to further studies.

5 References

- 1.- Hirschhorn, R; Reuser, AJJ. Glycogen storage disease type II: acid α -glucosidase (acid maltase) deficiency. In: Scriver, CR; Beaudet, AL; Sly, WS; Valle, D (Eds.). The metabolic and molecular bases of inherited disease, McGraw–Hill, New York, 2001, pp 3389–3420.
- 2.- Martiniuk, F; Chen, A; Mack, A; Arvanitopoulos, E; Chen, Y; Rom, WN; Codd, WJ; Hanna, B; Alcabes, P; Raben, N; Plotz, P. Am. J. Med. Genet. 1998, 79, 69–72.
- 3.- (a) Kishnani PS, Corzo D, Nicolino M, et al. Neurology, 2007, 68, 99–109.
(b) <http://www.myozyme.com/>
- 4.- <http://www.rxlist.com/myozyme-drug.htm>
- 5.- <http://en.wikipedia.org/wiki/Myozyme>.
- 6.- (a) Raben, N; Plotz, P; Byrne, BJ. Curr. Mol. Med., 2002, 2, 145–166.
(b) <http://www.hgmd.cf.ac.uk>
- 7.- (a) Montalvo, AL; Cariati, R; Deganuto, M; Guerci, V; Garcia, R; Ciana, G; Bembi, B; Pittis, MG. Mol. Genet. Metab., 2004, 81, 203–208. (b) Hermans, MM; van Leenen, D; Kroos, MA; Beesley, CE; Van der Ploeg, AT; Sakuraba, H; Wevers, R; Kleijer, W; Michelakakis, H; Kirk, EP; Fletcher, J; Bosshard, N; Basel-Vanagaite, L; Besley, G; Reuser, AJ. Hum. Mutat., 2004, 23, 47–56. (c) Reuser, AJ; Kroos, M; Willemsen, R; Swallow, D; Tager, JM; Galjaard, H. J. Clin. Invest., 1987, 79, 1689–1699. (d) Reuser, AJ; Kroos, M; Oude Elferink, RP; Tager, JM. J. Biol. Chem., 1985, 260, 8336–8341.
- 8.- (a) Beck, M. Human Genetics., 2007, 121, 1-22, (b) Horne, G; Wilson, FX.; Tinsley, J; Williams, DH; Storer, R; Drug Discov. Today, 2011, 16(3-4), Pages 107-118.

- 9.- (a) Parenti, G; Zuppaldi, A; Pittis, GM; Tuzzi, MR; Annunziata, I; Meroni, G; Porto, C; Donaudy, F; Rossi, B; Rossi, M; Filocamo, M; Donati, A; Bembi, B; Ballabio, A; Andria, G, Mol. Ther., 2007, 15, 508–514. (b) Okumiya, T; Kroos, MA; Vliet, LV; Takeuchi, H; Van der Ploeg, AT; Reuser, AJ. Mol. Genet. Metab., 2007, 90, 49–57.
- 10.- Jian-Qiang, F; Satoshi, I. The FEBS J., 2007, 274, 4962-71.
- 11.- Motabar, O; Shi, Z; Goldin, E; Liu, K; Southall, N; Sidransky, E; Austin, CP; Griffiths, GL; Zheng, Z. Anal. Biochem., 2009, 390, 79–84.
- 12.- (a) John, M; Wendeler, M; Heller, M; Sandhoff, K; Kessler, H. Biochemistry, 2006, 45, 5206–5216. (b) Zwerschke, W; Mannhardt, B; Massimi, P; Nauenburg, S; Pim, D; Nickel, W; Banks, L; Reuser, AJ; Jansen-Dürr, P., J. Biol. Chem., 2000, 275, 9534–9541.
- 13.- Parenti, G; Zuppaldi, A; Gabriela, PM; Rosaria, TM; Annunziata, I; Meroni, G; Porto, C; Donaudy, F; Rossi, B; Rossi, M; Filocamo, M; Donati, A; Bembi, B; Ballabio, A; Andria, G, Mol Ther. 2007, 15(3), 508-14.
- 14.- Okumiya, T; Kroos, MA; Van Vliet, L; Takeuchi, H; Van der Ploeg , AT; Reuser, AJJ, Molecular Genetics and Metabolism, 2007, 90, 49–57.
- 15.- Marugan, JJ; Zheng, W; Motabar, O; Southall, N; Goldin, E; Sidransky, E; Aungst, RA; Liu, K; Sadhukhan, SK; Austin, C, Eur. J. Med. Chem, 2010, 45, 1880-97.

Appendix

Pharmacokinetics protocol and levels

Study Design							
Treatment Group	Treatment	No. of animals	Route of admin.	Dose Level (mg/kg)	Dose Conc. (mg/mL)	Dose Volume (mL/kg)	Time points
1	NCGC00183885-01	30	IP	50	5	10	Predose, 0.083, 0.25, 0.5, 1, 2, 4, 8, 12 and 24 hr, plasma, brain, liver and heart collection

Test article	NCGC00183885-01
Test system	C57BL/6 mice, 15-20 g, male, N=30, purchased from SLAC Laboratory Animal Co. LTD Qualification No.: SCXK (SH) 2007-0005 20703
Food status	Free access to food and water
Administration	IP: 50 mg/kg (10 mL/kg) in 10% DMAC+10% Tetraethylene glycol+ 10% Solutol HS 15+ 70% Water via lower left abdominal quadrant injection (N=30)
Blood collection	The animals were anesthetized with isoflurane and restrained manually at the designated time points. Approximately 300 µL of blood samples were taken from the animals into K ₂ EDTA tube via cardiac puncture. Blood samples were put on ice and centrifuged to obtain plasma sample (2000 g, 5 min under 4 °C) within 15 minutes post sampling.
Heart collection	Perfusion: The animal was euthanized by exsanguination. The blunt syringe was held in place with a hemostat in the left ventricle for systemic perfusion. Cut the right auricle open to allow the blood to flow out. Perfuse the animals with cold saline (around 20 mL per animal) for a few minutes until blood is flushed. After the perfusion, the tissues were collected: Heart collection: Grasp the heart using a pair of ring forceps and cut above the right and left atrium. Place the heart on a piece of gauze, and then cut from the base to the apex in four sections to expose all the ventricles and atrium, rinsed with cold saline, dried on filtrate paper, weighed and snap frozen by placing into dry-ice.
Liver collection	Holding the liver lobes with forceps, and a pair of dissection scissors was used to separate the liver. The whole liver was collected, rinsed with cold saline, dried on filtrate paper, weighed and snap frozen by placing into dry-ice.
Brain collection	A mid-line incision was made in the animals scalp and skin retracted. The skull overlying the brain was removed. The whole brain was collected, rinsed with cold saline, dried on filtrate paper, weighed and snap frozen by placing into dry-ice.
Sample storage and disposition	Plasma, brain, liver and heart samples were stored at approximately -80 °C until analysis. The backup samples will be discarded after one month unless requested.

Individual and mean plasma concentration-time data of NCGC00183885-01 after an IP dose of 50 mg/kg in male C57BL/6 mice									
Dose (mg/kg)	Dose route	Sampling time (hr)	Concentration (ng/mL)			Mean (ng/mL)	Mean (µM)	SD	CV(%)
			Individual						
50	IP	0	BQL	BQL	BQL	BQL	BQL	NA	NA
		0.083	24100	22300	25000	23800	63.219	1375	5.78
		0.25	29700	29100	36100	31633	84.026	3880	12.3
		0.5	21600	25500	28300	25133	66.761	3365	13.4
		1	10300	16500	11300	12700	33.734	3329	26.2
		2	3090	3270	2970	3110	8.261	151	4.86
		4	1150	566	1180	965	2.564	346	35.9
		8	142	319	467	309	0.822	163	52.6
		12	157	37.6	13.3	69.3	0.184	76.9	111
		24	5.76	6.27	5.79	5.94	0.016	0.286	4.82
PK parameters		Unit	Estimate						
	T _{max}	hr	0.250						
	C _{max}	ng/mL	31600						
	Terminal t _{1/2}	hr	2.75						
	AUC _{last}	hr*ng/mL	37900						
	AUC _{INF}	hr*ng/mL	37900						

Table 7. Plasma pharmacokinetics in mouse of probe molecule **ML247** (NCGC00183885-01 in the image) upon single bolus IP administration of 50 mg/kg.

Individual and mean liver concentration-time data of NCGC00183885-01 after an IP dose of 50 mg/kg in male C57BL/6 mice									
Dose (gr/kg)	Dose route	Sampling time (hr)	Concentration (ng/g)			Mean (ng/g)	Mean (uM)	SD	CV(%)
			Individual						
50	IP	0	BQL	BQL	BQL	BQL	BQL	NA	NA
		0.083	60000	48800	72900	60567	160.880	12060	19.9
		0.25	39900	46000	34200	40033	106.339	5901	14.7
		0.5	32100	38000	42700	37600	99.875	5311	14.1
		1	13900	22400	19700	18667	49.583	4343	23.3
		2	5380	5330	5150	5287	14.043	121	2.29
		4	1060	1290	1230	1193	3.170	119	10.0
		8	207	258	278	248	0.658	36.6	14.8
		12	103	54.3	18.3	58.5	0.155	42.5	72.6
		24	11.7	10.1	61.2	27.7	0.073	29.1	105
PK parameters		Unit	Estimate						
T _{max}		hr	0.083						
C _{max}		ng/mL	60600						
Terminal t _{1/2}		hr	2.07						
AUC _{liver} (AUC _{last})		hr*ng/mL	57200						
AUC _{INF}		hr*ng/mL	57200						
AUC _{liver} /AUC _{plasma}		%	151						

Table 8. Liver pharmacokinetics in mouse of probe molecule **ML247** (called NCGC00183885-01 in the image) upon single bolus IP administration of 50 mg/kg.

Individual and mean heart concentration-time data of NCGC00183885-01 after an IP dose of 50 mg/kg in male C57BL/6 mice									
Dose (gr/kg)	Dose route	Sampling time (hr)	Concentration (ng/g)			Mean (ng/g)	Mean (uM)	SD	CV(%)
			Individual						
50	IP	0	BQL	BQL	BQL	BQL	BQL	NA	NA
		0.083	10000	10900	10000	10300	27.359	520	5.04
		0.25	11200	11300	13300	11933	31.698	1185	9.93
		0.5	12300	11300	11100	11567	30.724	643	5.56
		1	4630	7210	4510	5450	14.477	1525	28.0
		2	1080	1610	1640	1443	3.834	315	21.8
		4	317	244	218	260	0.690	51.3	19.8
		8	39.5	48.0	64.5	50.7	0.135	12.7	25.1
		12	29.3	14.1	8.23	17.2	0.046	10.9	63.2
		24	BQL	BQL	14.1	14.1	0.037	NA	NA
PK parameters		Unit	Estimate						
T _{max}		hr	0.250						
C _{max}		ng/mL	11900						
Terminal t _{1/2}		hr	2.34						
AUC _{heart} (AUC _{last})		hr*ng/mL	15600						
AUC _{INF}		hr*ng/mL	15600						
AUC _{heart} /AUC _{plasma}		%	41.2						

Table 9. Heart pharmacokinetics in mouse of probe molecule **ML247** (called NCGC00183885-01 in the image) upon single bolus IP administration of 50 mg/kg.

Individual and mean brain concentration-time data of NCGC00183885-01 after an IP dose of 50 mg/kg in male C57BL/6 mice									
Dose (gr/kg)	Dose route	Sampling time (hr)	Concentration (ng/g)			Mean (ng/g)	Mean (uM)	SD	CV(%)
			Individual						
50	IP	0	BQL	BQL	BQL	BQL	BQL	NA	NA
		0.083	572	534	472	526	1.397	50.5	9.60
		0.25	523	808	859	730	1.939	181	24.8
		0.5	712	776	708	732	1.944	38.2	5.21
		1	216	386	193	265	0.704	105	39.8
		2	52.6	48.7	54.5	51.9	0.138	2.96	5.69
		4	7.58	5.81	BQL	6.70	0.018	NA	NA
		8	BQL	BQL	BQL	BQL	BQL	NA	NA
		12	BQL	BQL	BQL	BQL	BQL	NA	NA
24	BQL	BQL	BQL	BQL	BQL	NA	NA		
PK parameters		Unit	Estimate						
T_{max}		hr	0.500						
C_{max}		ng/mL	732						
Terminal $t_{1/2}$		hr	0.579						
$AUC_{brain}(AUC_{last})$		hr*ng/mL	776						
AUC_{INF}		hr*ng/mL	781						
AUC_{brain}/AUC_{plasma}		%	2.05						

Table 10. Brain pharmacokinetics in mouse of probe molecule **ML247** (called NCGC00183885-01 in the image) upon single bolus IP administration of 50 mg/kg.